Prepared for submission to JHEP

Spectrum-doubled Heavy Vector Bosons at the LHC

Thomas Appelquist,[a] **Yang Bai,**[b] **James Ingoldby,**[a] **Maurizio Piai**[c]

[a] *Department of Physics, Sloane Laboratory, Yale University, New Haven, Connecticut 06520, USA*

[b] *Department of Physics, University of Wisconsin-Madison, Madison, WI 53706, USA*

[c] *Department of Physics, College of Science, Swansea University, Singleton Park, SA2 8PP, Swansea, Wales, UK*

Abstract: We study a simple effective field theory incorporating six heavy vector bosons together with the standard-model field content. The new particles preserve custodial symmetry as well as an approximate left-right parity symmetry. The enhanced symmetry of the model allows it to satisfy precision electroweak constraints and bounds from Higgs physics in a regime where all the couplings are perturbative and where the amount of fine-tuning is comparable to that in the standard model itself.

We find that the model could explain the recently observed excesses in di-boson processes at invariant mass close to 2 TeV from LHC Run 1 for a range of allowed parameter space. The masses of all the particles differ by no more than roughly 10%. In a portion of the allowed parameter space only one of the new particles has a production cross section large enough to be detectable with the energy and luminosity of Run 1, both via its decay to WZ and to Wh, while the others have suppressed production rates. The model can be tested at the higher-energy and higher-luminosity run of the LHC even for an overall scale of the new particles higher than 3 TeV.

Contents

1 Introduction

Recent analyses of 8-TeV data by the ATLAS and CMS collaborations show a $2-3\sigma$ excess in the production of high-mass, WW, WZ, ZZ as well as Wh pairs at about 2-TeV invariant mass [1, 2]. Inspired by these tentative signals of resonant production, we examine a simple effective field theory (EFT) that combines the standard model (SM) with a minimal set of spin-one states at the 2-TeV scale. It describes the coupling of these states to the longitudinal W and Z gauge bosons and the Higgs boson with a strength that can range from electroweak upward, leading to total resonance widths ranging from tens of GeV to a few hundred GeV. The coupling to the heavy states is then limited to a perturbative range by precision measurements of standard-model parameters, for example the Higgs-W-W coupling. This restriction, in turn, insures that the fine tuning required to keep the Higgs mass light is no worse than in the standard model itself.

EFTs of this type have been examined before [3–5]. They can arise in various contexts, including little-Higgs theories [6], extra-dimensional theories [7], and possibly walking technicolor theories [8] and theories of extended hidden local symmetry [9]. Here, we adopt a minimalist approach: we focus on symmetric setup in which six new vector bosons fill out a representation of a new $SU(2)_{L'} \times SU(2)_{R'}$ symmetry. We impose on the EFT a parity symmetry broken only by the standard-model interactions and we introduce only a minimal set of new couplings required to describe di-boson resonant behavior. This naturally restricts the electroweak precision parameters to within current bounds. Higgs boson decay widths remain in agreement with experiment provided that the coupling strength of the new vector bosons is in the range for which we can reasonably trust perturbation theory.

We devote Sections 2–5 to introducing the model and deriving and discussing analytical expressions for the physically relevant quantities. In Section 2, we describe the EFT including its mass parameters and couplings. In Section 3, we describe the constraints on the couplings arising from the precision measurement of processes involving standard-model particles. The decay widths of the new, heavy resonances are discussed in Section 4, and the fine tuning required to maintain the Higgs mass at 125 GeV is described in Section 5. In Section 6 we perform a numerical study of the properties of the model. In particular we compute LHC production cross sections for the new resonances and show that the model could explain excesses such as those possibly seen at LHC Run 1. We summarize and discuss our findings in Section 7.

2 The Effective Field Theory

The ingredients of our EFT are listed in Table 1. The columns and the moose diagram at the top correspond to the global symmetry group $SU(2)_L \times SU(2)_{L'} \times SU(2)_{R'} \times SU(2)_R \times U(1)_{B-L}$, in which the $SU(2)_L \times SU(2)_{L'} \times SU(2)_{R'} \times U(1)_Y$ subgroup is gauged. The hypercharge $Y = T^3 + \frac{1}{2}(B-L)$ is a combination of the T^3 generator of the $SU(2)_R$ group and $U(1)_{B-L}$. We write the gauge-boson field $B_\mu \equiv B^3_\mu[T^3 + \frac{1}{2}(B-L)]$. The gauge fields of $SU(2)_L$ are $W_\mu \equiv W^a_\mu T^a$. The additional vector fields are $L_\mu \equiv L^a_\mu T^a$ and $R_\mu \equiv R^a_\mu T^a$. The normalization is $\mathrm{Tr}\left[T^a T^b\right] = \delta^{ab}/2$.

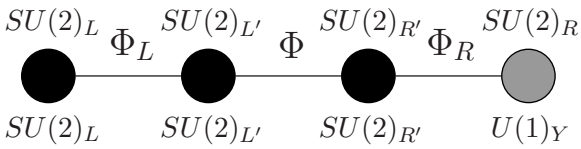

Fields	$SU(2)_L$	$SU(2)_{L'}$	$SU(2)_{R'}$	$SU(2)_R$	$U(1)_{B-L}$	$U(1)_Y$
Φ_L	2	2	1	1	0	0
Φ	1	2	2	1	0	0
Φ_R	1	1	2	2	0	$\pm 1/2$
q_L	2	1	1	1	$1/3$	$1/6$
q_R	1	1	1	2	$1/3$	$1/6 \pm 1/2$
ℓ_L	2	1	1	1	-1	$-1/2$
ℓ_R	1	1	1	2	-1	$-1/2 \pm 1/2$
W_μ	3	1	1	1	0	0
L_μ	1	3	1	1	0	0
R_μ	1	1	3	1	0	0
B_μ	1	1	1	$*$	0	0

Table 1. Diagramatic representation and field content of the model. In the figure, the global symmetries are on the top, the gauge symmetries on the bottom. The hypercharge is $Y = T^3 + \frac{1}{2}(B-L)$, with T^3 the generator of the $SU(2)_R$ group. The fields Φ_L, Φ and Φ_R are complex scalars, the quarks q_i and leptons ℓ_i are Weyl spinors, while W_μ, L_μ, R_μ and B_μ are gauge bosons. We complete the lepton doublet by adding right-handed neutrinos, which are singlets under all the gauge symmetries and hence inert. The $*$ highlights the fact that we gauge only the $U(1)_Y$ subgroup of $SU(2)_R \times U(1)_{B-L}$, which implies that the individual B_μ gauge boson transforms as incomplete representation of $SU(2)_R$. The presence of B_μ explicitly breaks the global $SU(2)_R$ symmetry.

The Lagrangian for the bosons, including operators up to dimension 4, is

$$\begin{aligned}\mathcal{L}_b = &+2g\mathrm{Tr}W^\mu J_{L\,\mu} + 2g'\mathrm{Tr}B^\mu J_{Y\,\mu} \\ &-\frac{1}{2}\mathrm{Tr}W_{\mu\nu}W^{\mu\nu} - \frac{1}{2}\mathrm{Tr}L_{\mu\nu}L^{\mu\nu} - \frac{1}{2}\mathrm{Tr}R_{\mu\nu}R^{\mu\nu} - \frac{1}{2}\mathrm{Tr}B_{\mu\nu}B^{\mu\nu} \\ &+\frac{1}{4}\mathrm{Tr}|D\Phi_L|^2 + \frac{1}{4}\mathrm{Tr}|D\Phi|^2 + \frac{1}{4}\mathrm{Tr}|D\Phi_R|^2 - V(\Phi_i)\,.\end{aligned} \tag{2.1}$$

The field strength tensors are defined so that the gauge bosons are canonically normalized and we denote with g, g_L, g_R and g' the four gauge couplings. $J_{L\mu}$ and $J_{Y\mu}$ are electroweak matter currents bilinear in the SM fermion fields. Their mass terms will be discussed later. The covariant derivatives for the scalars are

$$\begin{aligned}D_\mu\Phi_L &\equiv \partial_\mu\,\Phi_L - i\,(g\,W_\mu\,\Phi_L - g_L\,\Phi_L L_\mu)\,, \\ D_\mu\Phi &\equiv \partial_\mu\,\Phi - i\,(g_L\,L_\mu\,\Phi - g_R\,\Phi R_\mu)\,, \\ D_\mu\Phi_R &\equiv \partial_\mu\,\Phi_R - i\left(g_R\,R_\mu\,\Phi_R - g'\,\Phi_R B_\mu\right)\,.\end{aligned} \tag{2.2}$$

We write the potential for the scalars in the following way:

$$V = \frac{\lambda_L}{16}\left(\mathrm{Tr}\left[\Phi_L\Phi_L^\dagger - F_L^2\,\mathbb{I}_2\right]\right)^2 + \frac{\lambda}{16}\left(\mathrm{Tr}\left[\Phi\Phi^\dagger - f^2\,\mathbb{I}_2\right]\right)^2 + \frac{\lambda_R}{16}\left(\mathrm{Tr}\left[\Phi_R\Phi_R^\dagger - F_R^2\,\mathbb{I}_2\right]\right)^2 , \tag{2.3}$$

which means we do not include mixing terms in the potential between the scalars. These will be loop generated, and potentially require fine tuning, but in the coupling-strength range allowed phenomenologically this will be less than the amount of fine tuning we discuss in Section 5.

Taking $\lambda_L = \lambda_R$, $F_L = F_R \equiv F$ and $g_L = g_R = g_V$, the EFT is left-right symmetric, except for the weak gauging g and g' of the SM groups $SU(2)_L$ and $U(1)_Y$. The coupling strength g_V is a free parameter that we will allow to range from electroweak strength to $\mathcal{O}(4\pi)$. The potential induces symmetry breaking at the scale F in the case of Φ_L and Φ_R, at the scale f in the case of Φ, and consequently generates the electroweak scale $v_W \simeq 246$ GeV.

The bifundamental Φ describes the Nambu-Goldstone bosons (NGBs) associated with the scale f along with the physical Higgs particle h. The bifundamentals Φ_L and Φ_R play a similar role with respect to the scale F. Altogether the NGBs provide longitudinal components for all the gauge fields except for the massless photon. For simplicity, we take $\lambda_L = \lambda_R \to \infty$, freezing out the corresponding physical scalars and imposing the nonlinear constraints $\Phi_L\Phi_L^\dagger = F^2\,\mathbb{I}_2 = \Phi_R\Phi_R^\dagger$. In unitary gauge we replace $\Phi_L = F\,\mathbb{I}_2 = \Phi_R$ and $\Phi = (f+h)\,\mathbb{I}_2$, with h the (real and canonically normalized) Higgs field.

The 4×4 mass matrix for the neutral vector bosons in the basis $(W^\mu, L^\mu, R^\mu, B^\mu)$ is

$$\mathcal{M}_0^2 = \frac{1}{4}\begin{pmatrix} g^2F^2 & -gg_VF^2 & 0 & 0 \\ -gg_VF^2 & g_V^2(f^2+F^2) & -g_V^2f^2 & 0 \\ 0 & -g_V^2f^2 & g_V^2(f^2+F^2) & -g'g_VF^2 \\ 0 & 0 & -g'g_VF^2 & g'^2F^2 \end{pmatrix}, \tag{2.4}$$

while the 3×3 mass matrix $\mathcal{M}_+^2$ for the charged vectors can be obtained by removing the last row and column.

The eigenvalue structure of the 3×3 charged-vector mass matrix depends on the two ratios g^2/g_V^2 and f^2/F^2, where $g \approx 0.6$. The lightest eigenvalue is fixed to be $M_W = 80.4$ GeV and the next to lightest eigenvalue M_{V_1} is taken to be at least of order 2000 GeV. In this range, at least one of the two ratios g^2/g_V^2 or f^2/F^2 must be small.

We next exhibit explicitly the mass eigenvalues of the charged sector. With some abuse of notation, we denote the mass eigenstate W^+ with the same symbol as the original interaction eigenstate, though it results from mixing with the heavy vectors. In the regime $g \ll g_V$ the eigenvalues are given by the following relations:

$$M_{W^+}^2 \simeq \frac{1}{4}g^2\frac{f^2F^2}{F^2+2f^2}, \qquad M_{V_1^+}^2 \simeq \frac{1}{8}(2g_V^2+g^2)F^2,$$
$$M_{V_2^+}^2 \simeq \frac{1}{4}g_V^2(F^2+2f^2) + \frac{1}{8}g^2\frac{F^4}{F^2+2f^2}, \tag{2.5}$$

and the heavy eigenstates for all charge assignments are given by $V_1 \simeq (L+R)/\sqrt{2}$, and $V_2 \simeq (L-R)/\sqrt{2}$. In the regime $f \ll F$, we find

$$M^2_{W^+} \simeq \frac{1}{4}\frac{g^2 g_V^2}{g^2+g_V^2} f^2\,, \quad M^2_{V_1^+} \simeq \frac{1}{4} g_V^2 (F^2+f^2)\,,$$
$$M^2_{V_2^+} \simeq \frac{1}{4}(g_V^2+g^2)F^2 + \frac{1}{4}\frac{g_V^4}{g^2+g_V^2} f^2\,, \tag{2.6}$$

where $V_1^+ \simeq R^+$ and $V_2^+ \simeq (gW^+ - g_V L^+)/\sqrt{g^2+g_V^2}$.

For the neutral gauge bosons, in addition to the massless photon and Z boson, there are two heavy states V_1^0 and V_2^0 with masses nearly degenerate with their charged counterparts in the parameter range of interest. We exhibit here only an approximate expression for the mass of V_1^0, valid for $f \ll F$:

$$M^2_{V_1^0} = \frac{1}{4}\left[g_V^2(F^2+f^2) + g'^2(F^2-f^2)\right]\,, \tag{2.7}$$

where approximately $V_1^0 \simeq (g'B - g_V R^0)/\sqrt{g'^2+g_V^2}$.

To describe fermion masses in our model, we note that the combination $\Phi_L \Phi \Phi_R$ transforms as the Higgs field in the standard model. Hence we include the terms

$$\mathcal{L}_f = -\frac{1}{\sqrt{2}F^2}\bar{q}_L \Phi_L \Phi \Phi_R t_q q_R - \frac{1}{\sqrt{2}F^2}\bar{\ell}_L \Phi_L \Phi \Phi_R t_\ell \ell_R + \text{h.c.}\,, \tag{2.8}$$

where $t_q = \begin{pmatrix} y_t & 0 \\ 0 & y_b \end{pmatrix}$, $t_\ell = \begin{pmatrix} y_\tau & 0 \\ 0 & y_3 \end{pmatrix}$ and we show explicitly only the third standard-model family. There are also fermion kinetic terms with covariant derivatives as dictated by the quantum numbers of Table 1. Having imposed the nonlinear constraints on Φ_L and Φ_R and working in unitary gauge, these terms yield directly fermion mass expressions such as $m_t = y_t f/\sqrt{2}$ along with corresponding formulae for the bottom quark, τ lepton and third-generation neutrino ν_3. The relation between the VEV f and the electroweak scale will be described in the next section. The generalization to three standard-model families with CKM flavor mixing is straightforward. There remains one scalar field h in the spectrum with mass $m_h^2 = 2\lambda f^2$, which we identify as the the particle discovered by ATLAS [10] and CMS [11] with mass $m_h \approx 125$ GeV.

The fine-tuning necessary to stabilize the Higgs mass in the standard model remains an issue also for the current model. After determining the allowed range of parameters in the EFT, we conclude that the amount of fine-tuning needed is no worse than in the standard model itself.

3 Bounds from Standard Model Processes

We first discuss constraints from electroweak precision measurements. We then turn to constraints arising from the coupling of the Higgs boson to W pairs and from its decay to two photons.

Electroweak precision parameters can be discussed conveniently by examining the low-energy EFT written in terms of new gauge fields $\bar{V}^i = (\bar{W}^1, \bar{W}^2, \bar{W}^3, \bar{B})$ and their propagators, obtained by expanding about $q^2 = 0$ the two-point functions derived from Eq. (2.1). We focus on the transverse polarizations of the gauge bosons and on the coupling to the currents made of standard-model fermions:

$$\mathcal{L} = \frac{P_{\mu\nu}}{2}\bar{V}^{i,\mu}(-q)\bar{\pi}_{ij}(q^2)\bar{V}^{j,\nu}(q) + \tag{3.1}$$
$$\frac{\bar{g}}{2}\left[\bar{W}^{i\,\mu}(q)J_{L\,i\,\mu}(-q) + \bar{W}^{i\,\mu}(-q)J_{L\,i\,\mu}(q)\right] + \frac{\bar{g}'}{2}\left[\bar{B}^{\mu}(q)J_{Y\,\mu}(-q) + \bar{B}^{\mu}(-q)J_{Y\,\mu}(q)\right],$$

where $P^{\mu\nu} \equiv g^{\mu\nu} - q^\mu q^\nu/q^2$. The $\bar{\pi}_{ij}(q^2)$ functions can be expressed in terms of the parameters g, g', g_V, f and F. For our purposes, we will retain their q^2-dependence only up to $\mathcal{O}(q^2)$. We follow the conventions of Ref. [12], except that we rescale the gauge fields (and the gauge couplings $\bar{g}$ and $\bar{g}'$) such that $\bar{\pi}'_{33}(0) = 1 = \bar{\pi}'_{BB}(0)$.

All the information we need for universal precision electroweak constraints is contained in the functions $\bar{\pi}_{ij}(q^2)$ [12]: our model falls into this universal class because of the charge assignments of all the fields, in particular the fact that there are no direct couplings of the SM fermions to the $SU(2)_{L'} \times SU(2)_{R'}$ gauge bosons. [1] The $\hat{S}$ parameter, related to the S parameter by Peskin and Takeuchi [14] and the α_1 parameter of the EW chiral Lagrangian [15] as $\hat{S} = -\bar{g}^2\alpha_1 = \frac{\alpha}{4\sin^2\theta_W}S$, is defined with these conventions as

$$\hat{S} = \frac{\bar{g}}{\bar{g}'}\,\bar{\pi}'_{3B}(0)\,, \tag{3.2}$$

where $\bar{\pi}'$ indicates derivative of $\bar{\pi}$ in respect to q^2.

In the neutral sector, the function $\bar{\pi}(q^2)$ can be extracted from the matrix-valued functions $\pi^0(q^2) \equiv q^2\,\mathbb{I}_4 - \mathcal{M}_0^2$, written in the basis (W, L, R, B), by inverting $\pi^0(q^2)$, by retaining only the four corners of the result, by inverting again and finally by expanding in small-q^2. In the charged sector $\pi^+(q^2)$ is obtained by restricting to the first 3 rows and columns of $\pi^0(q^2)$, and the analogous $\bar{\pi}^+(q^2)$ for the charged sector is obtained by inverting the 11 element of $1/\pi^+$, and then again Taylor expanding in small-q^2 and truncating at $\mathcal{O}(q^2)$.

We will impose the bound $\hat{S} < 0.0039$. [2] The other universal precision parameters are discussed elsewhere [12], and we expect them to be suppressed as long as $g_V \gtrsim 1$. For our purposes we need only to stress that the T parameter does not receive important contributions, as the new gauge bosons preserve the $SU(2)_R$ custodial symmetry that is only broken by g' in the gauge sector (models in which custodial symmetry is not implemented can also be considered, as for instance suggested in [16]).

[1] Generalizations of the model in which fermions couple directly to the new gauge bosons require a more general formalism for electroweak precision physics [13].

[2] This is the 3σ bound for a light Higgs from [12], obtained in a global fit of all the precision parameters that includes 1-loop corrections from loops of SM fields, h and top quark in particular. The bound has to be taken as indicative since the loop-level analysis of SM radiative corrections, which must be included to establish an experimental limit on $\hat{S}$, will involve modified couplings.

The result for the $\hat{S}$ parameter is

$$\hat{S} = \frac{2f^2 g^2 \left(f^2 + F^2\right)}{{g_V}^2 \left(2f^2 + F^2\right)^2 + g^2 \left(2f^4 + 2f^2 F^2 + F^4\right)} \,. \tag{3.3}$$

Generically, this is $\mathcal{O}(1)$, but we have already noted that to accommodate the requirement $M_{V_1^+} \gtrsim 2000$ GeV, we must take either $g^2 \ll g_V^2$ or $f^2 \ll F^2$. For $g^2 \ll g_V^2$ this becomes

$$\hat{S} \simeq \frac{2f^2(f^2+F^2)g^2}{(2f^2+F^2)^2 g_V^2} \,, \tag{3.4}$$

which can also be derived in an alternative way that we summarize in Appendix A, while for $f^2 \ll F^2$ it becomes

$$\hat{S} \simeq \frac{2g^2 f^2}{(g_V^2+g^2)F^2} \,. \tag{3.5}$$

In either limit, the expressions for the $\hat{S}$ parameter can be combined with earlier expressions for the masses of the vector bosons, to conclude that throughout the parameter space $\hat{S} \lesssim 2M_W^2/M_{V_{1,2}}^2$. Thus for $M_{V_{1,2}} \gtrsim 2$ TeV one finds $\hat{S} \lesssim 0.003$. This has to do with the way in which we built the model itself: due to our set-up, *all* effects of new physics are suppressed by $\mathcal{O}(M_W^2/M_{V_i}^2)$ coefficients. [3] The same applies to other coefficients of the electroweak chiral Lagrangian at $\mathcal{O}(p^4)$, for which the bounds are weaker [17].

From the expression for the charged $\bar{\pi}^+(q^2)$ we can extract the Fermi constant, $G_F/\sqrt{2} \equiv 1/(2v_W^2)$, where $v_W \simeq 246$ GeV is given by

$$v_W^2 = \lim_{q\to 0} \frac{4}{\bar{g}^2}\left(q^2 - \bar{\pi}^+\right) = \frac{f^2F^2}{F^2+2f^2} \,. \tag{3.6}$$

The low energy effective theory includes also the Higgs h. The coupling of the Higgs to the fermions ψ is controlled by the fermion mass m_ψ

$$\mathcal{L}_f = \cdots - c\frac{h}{v_W} m_\psi \bar{\psi}\psi \,, \tag{3.7}$$

related to the SM prediction by the factor

$$c \equiv v_W/f \,. \tag{3.8}$$

The coupling of h to two W bosons is rescaled with respect to the standard-model coupling M_W^2/v_W by a multiplicative factor a. We find the approximate relations

$$a \simeq \begin{cases} \frac{F^3}{(F^2+2f^2)^{3/2}} = c^3 \,, & (g \ll g_V) \\ 1 - \frac{(2g^4+4g^2g_V^2+3g_V^4)f^2}{(g^2+g_V^2)^2F^2} \,, & (f \ll F) \end{cases} \,, \tag{3.9}$$

[3] For the precision parameters W and Y defined in Ref. [12], for $g_V \gtrsim 1$ we find the approximate relations $W \sim g^2/(4g_V^2)\hat{S}$ and $Y \sim g'^2/(4g_V^2)\hat{S}$, which make them further suppressed with respect to $\hat{S}$.

and analogous expressions hold for the coupling to two Z bosons. For any range of g/g_V, there is significant suppression of the Higgs coupling to the W bosons, relative to the standard model, unless $f \ll F$. We impose this restriction, ensuring compatibility with current data from ATLAS and CMS [19]. Then, as we will see in Section 6, maintaining a fixed ratio M_W/M_{V_1} leads to an upper bound on g_V.

A similar calculation yields the couplings a_1 and a_2 of the Higgs to the heavy vectors $V_1^\pm$ and $V_2^\pm$, all of which are suppressed. We do not report them here, but we find that these coefficients satisfy the sum rule $a + a_1 + a_2 = c$. This allows us to write the decay rate of the Higgs to two photons approximately as

$$\Gamma(h \to \gamma\gamma) = \frac{G_F \alpha^2 m_h^3}{128\sqrt{2}\,\pi^3} \left| c\, A_t(\tau_t) N_c N_f Q^2 \,+\, a\, A_W(\tau_W) \,+\, (c-a) A_W(0) \right|^2 , \quad (3.10)$$

where $A_t(\tau_t) \simeq 1.38$, $A_W(\tau_W) \simeq -8.3$, and $A_W(0) = -7$. The three terms represent the contribution of the top loop (which implies $N_c = 3$, $N_f = 1$ and $Q^2 = 4/9$), of the W loops and the loops of heavy charged vectors, respectively. For $a = c = 1$ this is the SM rate.

4 Decay Processes of Heavy Vectors

We take the masses of the heavy vector bosons of our EFT to be at least as large as suggested by the ATLAS and CMS di-boson excesses [1, 2]. Depending on parameter values, the masses of the six particles can be well split or nearly degenerate. In either case the dominant decays will be two-body, to either a pair of SM fermions or a pair of SM bosons. To determine the fermionic decay width of the charged vector states, we start from the full $\pi^+(q^2)$ matrix function in the (W, L, R) basis of our EFT, and make use of the replacement

$$\left(\frac{1}{q^2 - M_W^2}\right)_{\rm SM} \to \left(\frac{1}{\pi^+(q^2)}\right)_{WW} \quad (4.1)$$

$$\equiv \frac{4\left(F^2 g_V^2 - 4q^2\right)\left[g_V^2\left(2f^2 + F^2\right) - 4q^2\right]}{f^2 g_V^2\left[-g^2 g_V^2 F^4 + 8F^2 q^2\left(g^2 + g_V^2\right) - 32q^4\right] + 4q^2\left(F^2 g_V^2 - 4q^2\right)\left[F^2\left(g^2 + g_V^2\right) - 4q^2\right]} ,$$

$$\simeq \frac{r_W}{q^2 - M_W^2} + \frac{r_{V_1^+}}{q^2 - M_{V_1^+}^2} + \frac{r_{V_2^+}}{q^2 - M_{V_2^+}^2} , \quad (4.2)$$

in the relevant amplitude. The residues are approximately given by the following expressions, valid for $g \ll g_V$:

$$r_W \simeq 1 - \frac{g^2}{g_V^2}\left[1 - \frac{2f^2(f^2+F^2)}{(2f^2+F^2)^2}\right] , \quad r_{V_1^+} \simeq \frac{g^2}{2g_V^2} , \quad r_{V_2^+} \simeq \frac{g^2 F^4}{2g_V^2(2f^2+F^2)^2} , \quad (4.3)$$

while in the limit $f \ll F$ we have

$$r_W \simeq \frac{g_V^2}{g_V^2 + g^2} + \frac{2f^2 g^2 g_V^4}{F^2(g^2+g_V^2)^3} , \quad r_{V_1^+} \simeq \frac{g_V^2 f^4}{g^2 F^4} , \quad r_{V_2^+} \simeq \frac{g^2}{g_V^2 + g^2} - \frac{2f^2 g^2 g_V^4}{F^2(g^2+g_V^2)^3} \quad (4.4)$$

Both satisfy the sum rule $1 = r_W + r_{V_1^+} + r_{V_2^+}$. These approximations have to be used carefully: the two limits do not commute, as for instance taking the $g \to 0$ limit of the second set of approximations would yield an incorrect result.

The partial width of the charged gauge bosons into standard-model fermions can be obtained directly from the corresponding width of the W boson, with three modifications: the mass of the gauge bosons has to be replaced, the coupling is suppressed by $\sqrt{r_V}$, and all heavy fermions have to be included. The result for the decay of the charged heavy vectors to $e^+\nu_e$ is

$$\Gamma\left(V^+_{1,2} \to e^+\nu_e\right) = r_{V^+_{1,2}} \frac{g^2 M_{V^+_{1,2}}}{48\pi}\,, \tag{4.5}$$

and the total decay rate to SM fermions is $\Gamma\left(V^+_{1,2} \to \psi'\bar{\psi}\right) = 3(1+N_c)\Gamma\left(V^+_{1,2} \to e^+\nu_e\right)$. In the case of the neutral vectors, the analogue of Eq. (4.1) involves mixing matrices. We do not report the details, but we perform an exact numerical study later in the paper.

Because the masses of all the new spin-one states are much larger than the masses of the electroweak gauge bosons, the Goldstone boson equivalence theorem applies. Decay rates involving W and Z are dominated by the contribution of the longitudinally polarized particles, while we neglect the contribution of transverse polarizations. In a somewhat similar manner, the fact that the Higgs particle has a mass at least 15 times lighter than the new spin-one states means that decay rates involving the Higgs particle can be computed (at leading order) by setting $f = 0$. For these reasons we estimate the di-boson decay rates with $f = 0$, so that the relatively small amount of electroweak symmetry breaking is neglected.

The electroweak bosons in this limit are massless, and we reinstate all the degrees of freedom of Φ. We write

$$\Phi = \begin{pmatrix} h_0 + i h_3 & i h_1 + h_2 \\ i h_1 - h_2 & h_0 - i h_3 \end{pmatrix}\,, \tag{4.6}$$

with canonically normalized, real h_i. The couplings of the neutral, heavy spin-one states to the scalars are

$$\mathcal{L}_b = \cdots + \frac{g_V}{\sqrt{2}}\left[\frac{R^3+L^3}{\sqrt{2}}(h_1\partial h_2 - h_2\partial h_1) + \frac{R^3-L^3}{\sqrt{2}}(h_0\partial h_3 - h_3\partial h_0) + \cdots\right]\,. \tag{4.7}$$

In these approximations, the partial width (at leading order in $f \ll F$) is given by

$$\Gamma(V_1^+ \to \text{ di-bosons}) \simeq \frac{g_V^2}{96\pi} M_{V_1^+}\,. \tag{4.8}$$

For the other vector bosons, even in the $f = 0$ limit we must retain the mixing due to the gauge couplings, and find accordingly that

$$\Gamma(V_2^{+,0} \to \text{ di-bosons}) \simeq \left(\frac{g_V^2}{g_V^2+g^2}\right)\frac{g_V^2}{96\pi} M_{V_2^{+,0}}\,, \tag{4.9}$$

for both the charged and neutral vectors, and for the neutral state V_1^0

$$\Gamma(V_1^0 \to \text{ di-bosons}) \simeq \left(\frac{g_V^2}{g_V^2+g'^2}\right)\frac{g_V^2}{96\pi} M_{V_1^0}\,. \tag{4.10}$$

When the mass splitting is large enough, there exist also decays of the type $V_2 \to V_1 + h, X$, where X is a SM gauge boson. These decays contribute negligibly to the total width.

5 Fine Tuning

Before presenting phenomenological and numerical estimates, we discuss briefly the amount of fine tuning intrinsic to our model. As with any EFT, this discussion can provide only general guidance on the issue of fine tuning and the scale of new physics. A specific UV completion could modify the discussion. Nevertheless, an EFT-based discussion has the virtue of generality and it reveals some interesting features. The tree-level scalar potential reproduces the standard model. The general form of the one-loop potential in the external field language is

$$V_1 = \frac{\Lambda^2}{32\pi^2}\mathcal{STr}\,\mathcal{M}^2 + \frac{1}{64\pi^2}\mathcal{STr}\left[(\mathcal{M}^2)^2\left(\ln\frac{\mathcal{M}^2}{\Lambda^2} + c_i\right)\right], \tag{5.1}$$

where Λ is the UV cutoff, $\mathcal{STr}$ is a trace in which fermionic degrees of freedom have negative weight, $\mathcal{M}^2(h)$ is the second derivative of the interaction part of the Hamiltonian, evaluated for general h, and c_i are scheme-dependent and field-dependent constants.

In the standard model, the dominant quadratically divergent part of the potential contributes to the Higgs mass [18]

$$\Delta m_h^2(\mathrm{SM}) = \frac{\Lambda^2}{32\pi^2}\left[\frac{3}{2}(3g^2 + g'^2) + \frac{6m_h^2}{v_W^2} - \frac{24m_t^2}{v_W^2}\right] + \cdots . \tag{5.2}$$

For $m_h \simeq 125$ GeV, and $\Lambda \simeq 10 - 30$ TeV, this results in $|\Delta m_h^2| \simeq 2.5 - 25$ TeV^2. This necessitates a counter-term chosen with fine-tuning $\mathcal{Z} \equiv |m_h^2/\Delta m_h^2| \simeq 0.006 - 0.0006$.

In our model, for $f \simeq v_W$:

$$\Delta m_h^2 \simeq \frac{\Lambda^2}{32\pi^2}\left(9g_V^2 + \frac{6m_h^2}{v_W^2} - \frac{24m_t^2}{v_W^2}\right) + \cdots . \tag{5.3}$$

Notice that g and g' do not appear at this order, while they do in the log-divergent and finite corrections.

A comparison of these two expressions reveals that for $g_V \simeq g$, the magnitude and sign of required fine tuning are the same. For larger g_V, the possibility of some accidental cancellation with the top-quark term arises in our EFT. It would be almost exact for $g_V \simeq 1.05$. For the range $g_V \geq 2.0$, to emerge from our phenomenological study in the next section, the first term in Eq. (5.3) dominates, reversing the sign of the quadratically divergent contribution to Δm_h^2. For g_V not too far above 2.0, the magnitude of the required fine tuning is approximately the same as in the standard model.

6 Phenomenology and Numerical Study

We first look at the constraints on the model from precision electroweak physics and from the properties of the Higgs particle, and then at the signatures of the new particles in direct searches at high energies. We are mostly interested in the regime $f \ll F$, in which limits from electroweak precision tests are satisfied, in which the Higgs couplings are close to the standard model ones, and in which fine-tuning is at a comparable level with the standard model.

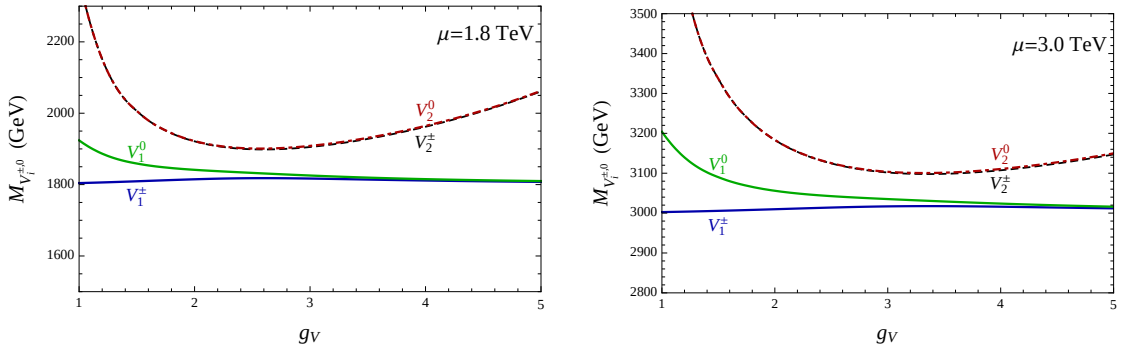

Figure 1. Mass spectrum (in GeV) of the heavy vector bosons in the model, as a function of g_V, for the choices of parameters discussed in the text. The left panel shows the masses for $\mu = 1.8$ TeV, the right panel for $\mu = 3.0$ TeV. The blue continuous curves show the mass of $V_1^\pm$, the black dashes line the mass of $V_2^\pm$, the green continuous lines show the mass of V_1^0 and the red dot-dashed line the mass of V_2^0.

There are five parameters, g, g', g_V, f and F. We keep fixed the indicative scale of the new particles $\mu \equiv \frac{1}{2} g_V F$. For each choice of g_V we then use Eq. (3.6), together with the exact diagonalization of the mass matrices in order to fix the parameters f, g and g' so that we reproduce the standard model values $M_W \simeq 80.4$ GeV, $M_Z \simeq 91.2$ GeV, $v_W \simeq 246$ GeV. With all of this in place, all the new physics depends on only one parameter, namely g_V. In the following, we make two representative choices $\mu = 1.8$ TeV and $\mu = 3.0$ TeV.

We compute the spectrum by diagonalizing numerically the mass matrices. The results are shown in Fig. 1. Notice that $V_2^\pm$ and V_2^0 are so close in mass that they appear as just one line (the heaviest mass). Their masses come close to the masses of the lighter V_1 bosons for intermediate values of g_V, but differ substantially both for large g_V and small g_V. While for large g_V one can choose f and F to be of similar order, when g_V becomes smaller one is forced towards the $f \ll F$ limit in which the masses of V_1 and V_2 become degenerate. But having kept μ fixed, as well as having imposed the requirement that the light masses agree with the standard-model bosons, the limit of small g_V is a limit in which the explicit breaking of the left-right symmetry due to the g and g' couplings is enhanced.

The mass of $V_1^\pm$ is approximately degenerate with V_1^0 for large g_V, but the degeneracy is lifted at small g_V. This charged-neutral splitting is due to the fact that the diagonalization of the mass matrix for the neutral vectors differs by effects that are controlled by the g' coupling. These effects are hence negligible when $g_V \gg g'$, but are enhanced when g_V is small.

6.1 Constraints from Indirect Searches

For the electroweak precision parameter $\hat{S}$, we use Eq. (3.3), and we show the results in the top left panel of Fig. 2. We also look at the couplings of the Higgs h, making use of the exact result for $c = v_W/f$ and numerical results for a.

The measurements of cross sections times decay rates of processes involving the Higgs place important bounds on our model parameter space. The processes in which a Higgs

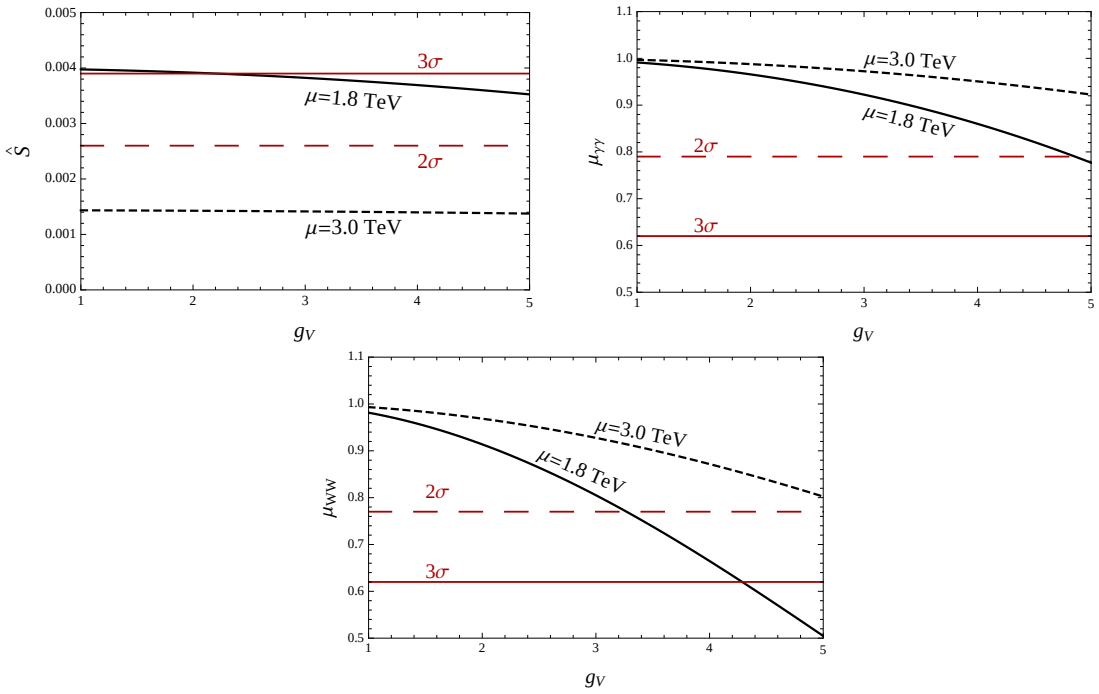

Figure 2. Bounds from indirect searches. The top left panel show $\hat{S}$ as a function of g_V, and for the choices of parameters described in the text (in black). The top right panel shows $\mu_{\gamma\gamma}$ for the same choices of parameters and the last panel shows μ_{WW}. The continuous lines are for $\mu = 1.8$ TeV, the dashed lines for $\mu = 3.0$ TeV. In all plots we compare to the 3σ (red) and 2σ (red long dashing) indicative bounds discussed in the text.

decays to W bosons or photons are particularly important. To derive these bounds, we look at the signal strength as measured by the ATLAS and CMS collaborations in Run 1. The signal strength μ_i is defined as the number of observed events of a given type i, normalized relative to the prediction from the standard model computed with Higgs mass $125 - 126$ GeV. Thus $\mu_i = 1$ indicates perfect agreement with the standard model. The use of the signal strength originates from the fact that the combined 2-parameter fits in [19], cannot be used, as our expression for the $h \to \gamma\gamma$ rate contains contributions from the heavy vector bosons, which are absent in the combination done by the experimental collaborations.

We compare the signal strength $\mu_{\gamma\gamma}$ to the weighted average of the signal strengths measured by CMS and ATLAS, that we find to be $\mu_{\gamma\gamma} = 1.13 \pm 0.17$ from [19], by making use of the rough approximation

$$\mu_{\gamma\gamma} \simeq \frac{c^2}{0.75\, c^2 \,+\, 0.25\, a^2} \, \frac{\Gamma(h \to \gamma\gamma)}{\Gamma(h \to \gamma\gamma)_{\rm SM}} \,, \tag{6.1}$$

together with Eq. (3.10).

This approximation for $h \to \gamma\gamma$ has the following origin (see also Appendix B). The factor of c^2 arises from the fact that the dominant production cross section comes from gluon-gluon fusion (ggF), in which the coupling of the Higgs particle to the gluons is due

to a loop of top quarks. The coupling of the Higgs to top quarks is suppressed in our model by a factor of c with respect to the standard model. The denominator is an approximation of the rescaling of the total width of the Higgs particle in our model: neglecting the small contribution from $\gamma\gamma$ itself. For $m_h \sim 125$ GeV in the standard model the branching ratio (BR) is approximately 75% in bb, cc, $\tau\tau$ and gg, all of which are suppressed as c^2, while 25% comes from decays into WW^* that are suppressed by a^2 with respect to the standard model, together with a smaller ZZ^* fraction, suppressed in a similar way. Finally the ratio of the $\gamma\gamma$ rate with respect to the standard model has been discussed earlier in the paper. Here and in the following c and a are computed numerically, without any of the approximations we discussed in Section 3.

Finally, we compare the signal strength μ_{WW} to the weighted average of CMS and ATLAS $\mu_{WW} = 1.07 \pm 0.15$ from [19], by making use of the rough approximation

$$\mu_{WW} \simeq \frac{c^2 a^2}{0.75\, c^2 \,+\, 0.25\, a^2}\,. \tag{6.2}$$

The results of both analysis are shown in Fig. 2, from which we deduce the bound $g_V \lesssim 4.2$ at 3σ. The behavior of the curves follows from the fact that for $f/F \to 0$ our EFT coincides with the standard model. In this limit $f \to v_W$ and hence $c = 1$. Because we keep $\mu = \frac{1}{2} g_V F$ fixed, this is the limit in which g_V becomes small. By contrast, taking g_V large for fixed μ means lowering F to the point where the modifications of the Higgs couplings become large, conflicting with the experimental bounds.

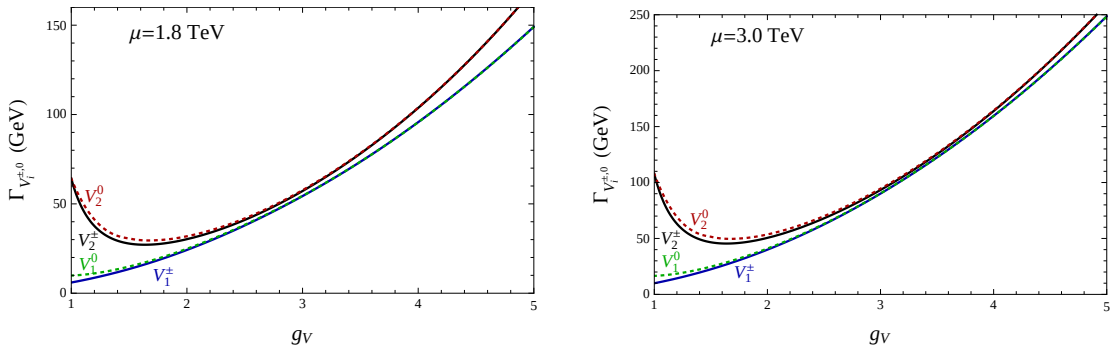

Figure 3. The total widths (in GeV) of the charged particles $V_1^\pm$ (blue), $V_2^\pm$ (black). V_1^0 (dashed, green) and V_2^0 (dashed, red). The left panel shows $\mu = 1.8$ TeV, the right panel $\mu = 3.0$ TeV.

6.2 Direct Searches

We next study the strength of the coupling to the currents J_L and J_Y. We do so by numerically computing the residues at the poles in the propagators for charged and neutral gauge bosons, as in Eq. (4.1). The results affect the production cross sections, as well as the partial widths of the particles. We do not report these intermediate results, except for commenting on the fact that we checked explicitly that the couplings of the physical W and

Z bosons reproduce the standard-model values, within the accuracy required by precision physics.

The widths of the heavy particles are shown in Fig. 3. The total widths include all the di-boson channels (computed with the equivalence theorem in Section 4) as well as the decay to all standard-model fermion pairs. The total widths range from tens of GeV to $100 - 200$ GeV. Because the width of the neutral particles is close to that of their charged partners, we focus our attention on the charged particles in this discussion. The width of the V_1^+ decreases as g_V is reduced for two reasons. Firstly, its bosonic width is proportional to g_V^2. Secondly, in the small g_V limit, the quantity f/F becomes small, and the V_1^+ becomes predominantly the R^+ state, as discussed in Section 2. Its coupling to fermion pairs is suppressed by the factor $r_{V_1^+}$ shown in Eq. (4.4). The bosonic width of the V_2^+ also decreases with g_V but then the width to fermion pairs kicks in. The mass eigenstate V_2^+ becomes a linear combination of L^+ and W^+ in this limit, and its fermionic width is not suppressed. This can be seen from the factor $r_{V_2^+}$ in Eq. (4.4). As a result, the width of V_2^+ has a minimum around $g_V \approx 1.5$.

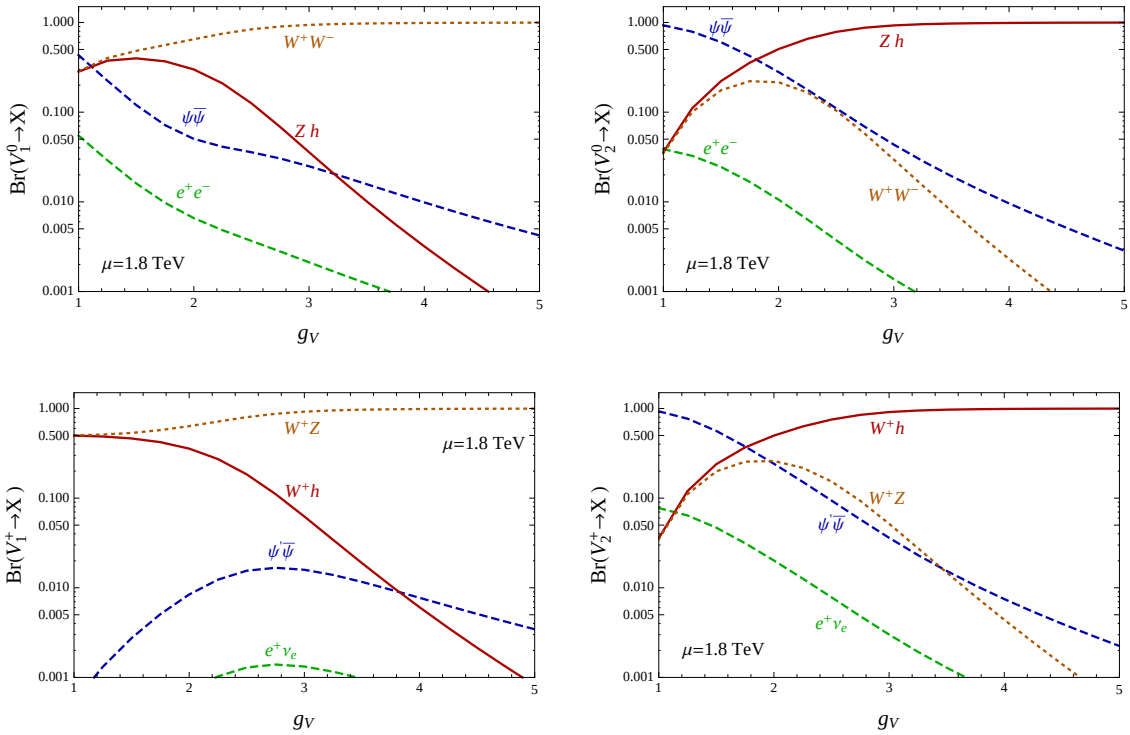

Figure 4. Branching fractions for $\mu = 1.8$ TeV. Top to bottom, left to right, the branching ratios of V_1^0, V_2^0, V_1^+ and V_2^+.

To provide more detail, we next look at the branching ratios of all the heavy particles, including the neutral ones, in Fig. 4 for $\mu = 1.8$ TeV. The branching fractions for $\mu = 3$ TeV have similar behavior and we do not show them. The suppressed branching fractions

of the heavy neutral and charged V_2 particles to V_1 particles and SM bosons have not been included in Fig. 4. For the V_1^+, the di-boson channels dominate the decay width throughout the exhibited g_V range due to the suppressed coupling to standard model fermions discussed above. For the V_1^0, the standard-model fermion channel is generally suppressed but becomes comparable to the di-boson channel for very small g_V. The reason is that in this limit the V_1^0 becomes a linear combination of R^0 and B, both of which couple to SM-fermion pairs with electroweak strength. For both the V_2^0 and V_2^+, which become linear combinations of L and W in the small-g_V limit, the SM-coupling to the fermions is somewhat stronger than for the V_1^0, so these modes dominate below $g_V \approx 1.5$. Each of these features has important consequences for the various production cross sections.

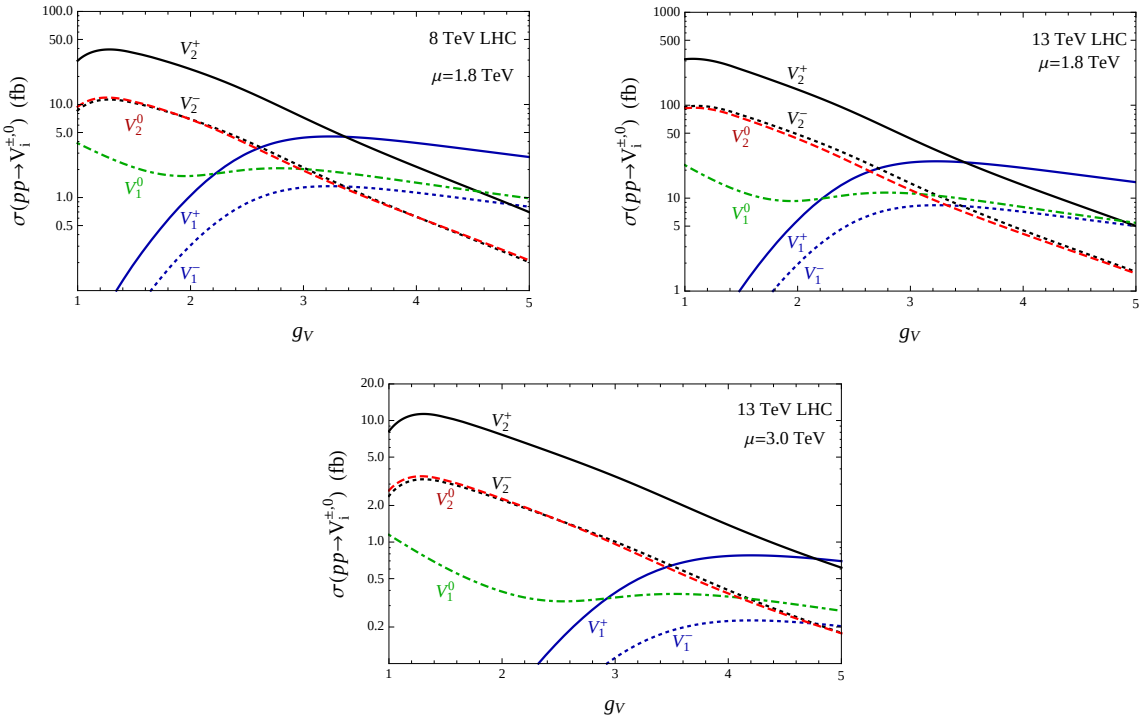

Figure 5. Production cross sections in Drell-Yan processes for the heavy vector bosons in pp collisions at $4 + 4$ TeV, for $\mu = 1.8$ TeV (top left) and at $6.5 + 6.5$ TeV for $\mu = 1.8$ TeV (top right) and $\mu = 3.0$ TeV (bottom).

In Fig. 5, we show the Drell-Yan (DY) production cross sections for the six heavy particles at both 8 TeV and 13 TeV at the LHC. The MSTW 2008 PDFs [20] have been used in our numerical calculations with the renormalization scale chosen to be the resonance mass. Following the strategy in [21], we have checked that the vector-boson-fusion (VBF) production cross sections are relatively suppressed, always below 1 fb, throughout the parameter range. In the pp collisions of the LHC, the negatively charged particles, which otherwise have the same properties as the positively charged ones, have smaller DY production cross sections. In the parameter range $g_V \lesssim 3$, where $f \ll F$, the production of the $V_1^\pm$ is strongly suppressed relative to the V_2. The reason is that $V_1^\pm \approx R^\pm$ in this

range, and is therefore not directly coupled to the quarks. At 8 TeV, the production of the V_1^0 is also suppressed relative to the V_2 due to the smallness of the neutral EW coupling relative to the charged EW coupling.

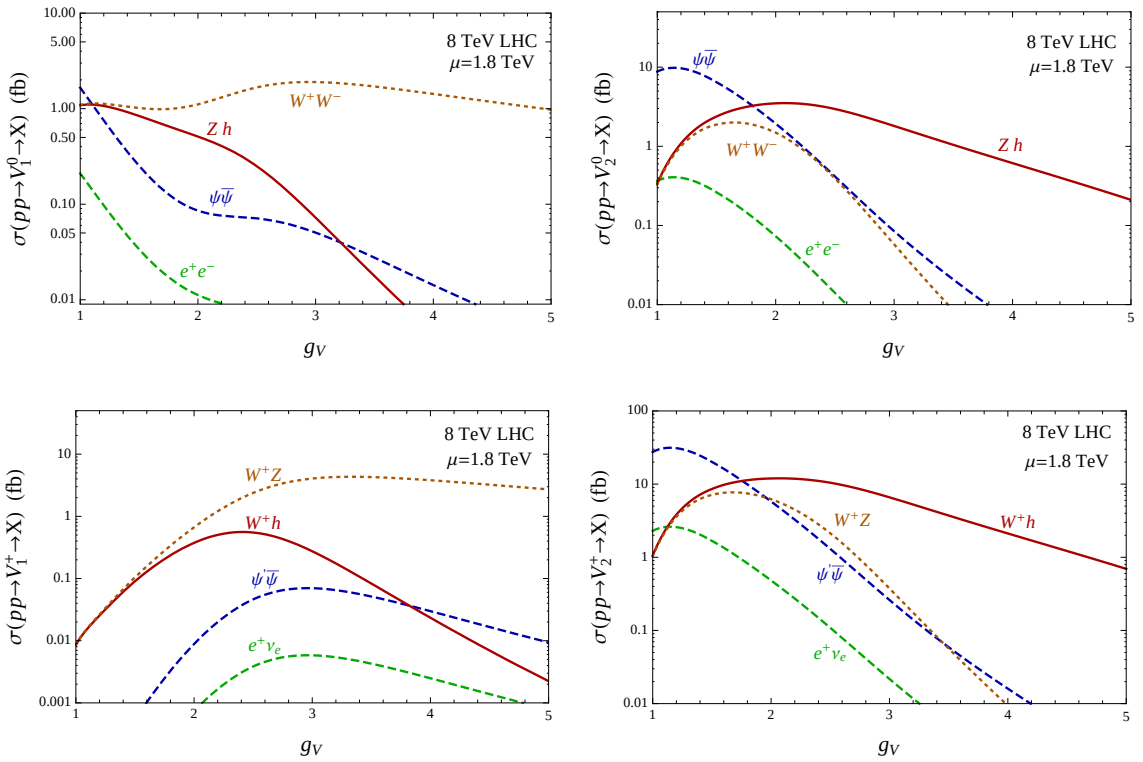

Figure 6. Cross section times branching fractions for the heavy particles, for $\mu = 1.8$ TeV for the 8 TeV LHC. The top-left panel shows V_1^0, top-right shows V_2^0, bottom-left shows V_1^+ and the bottom-right panel shows V_2^+.

In Fig. 6, we show cross sections times branching fractions for the case $\mu = 1.8$ TeV, for 8 TeV at the LHC. Results are shown for the V_2^+, which has the largest production cross section for much of the g_V range, as well as for the V_2^0, V_1^0 and V_1^+. First of all, by requiring that the cross section for $pp \to V_2^+ \to e^+\nu_e$ is bounded by $\sigma \times \text{BR} \lesssim 0.5$ fb [22], we deduce the approximate bound $g_V \gtrsim 2$. Similarly, by requiring that the cross section for $pp \to V_2^0 \to e^+e^-$ is bounded by $\sigma \times \text{BR} \leq 0.2$ fb [23], we deduce the approximate bound $g_V \gtrsim 1.6$.

We conclude that for $\mu = 1.8$ TeV, the bounds from standard-model processes and from direct searches involving new spin-one particles are satisfied provided that the coupling g_V is in the range

$$2.0 \lesssim g_V \lesssim 4.2\,, \tag{6.3}$$

with the lower bound being a 95% bound from direct searches, and the 3σ upper bound coming from $pp \to h \to WW$. The bounds on the $\hat{S}$ parameter are always satisfied at the 3σ level. We note that this allowed coupling range broadly agrees with the range emerging from a fit performed in Ref. [24] in the context of W' models.

In our allowed parameter range, and with $\mu = 1.8$ TeV, the mass of the V_2 is $1.9 - 2.0$ TeV while the mass of the V_1 is close to 1.8 TeV. Despite the relative heaviness of the V_2^+, it is its production and subsequent decay to WZ and Wh that could be prominent enough to explain the observed excess in Run 1 of the LHC, at least for g_V near the lower end of the above range $g_V \simeq 2$. The cross section times branching ratio in these two cases is $6 - 7$ fb and 10 fb respectively (see also the model-independent analysis in [25, 26]). The fact that this particle is degenerate with the V_2^0 and V_2^- yields a modest enhancement in these events. By contrast, for small g_V, the production of the V_1^0 and $V_1^\pm$ followed by di-boson decay is too small to be observable in Run 1 of the LHC.

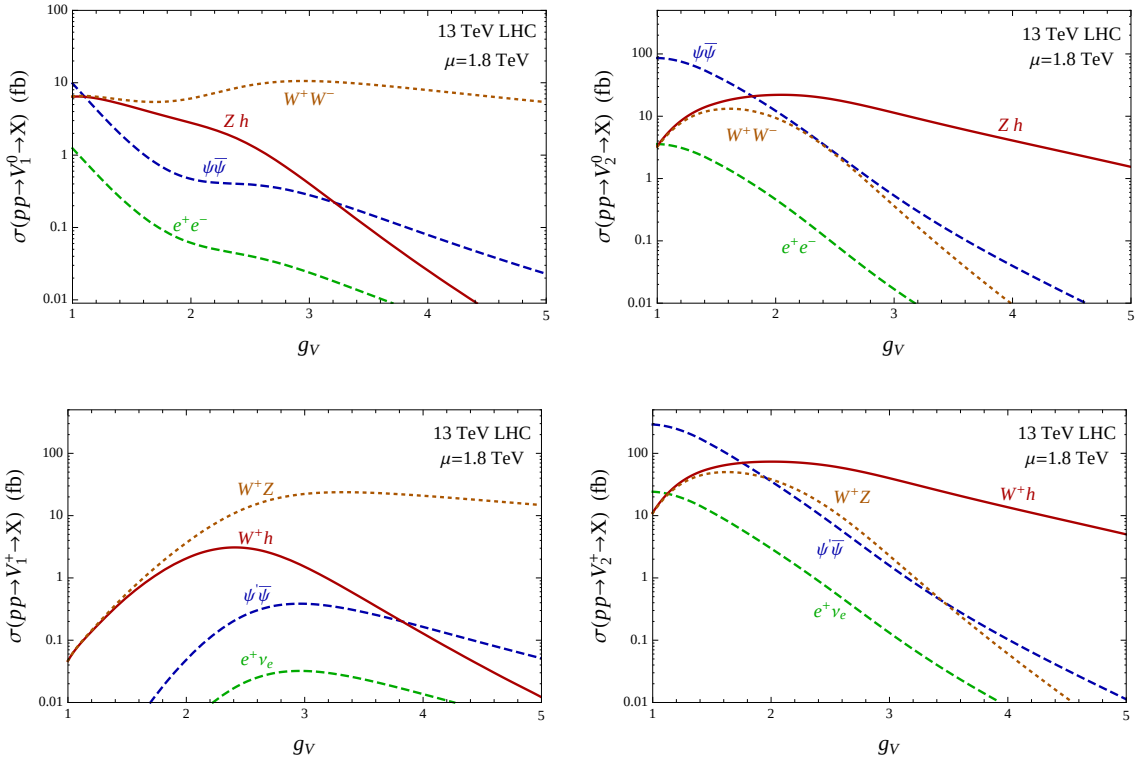

Figure 7. Cross section time branching fractions for the heavy particles, for $\mu = 1.8$ TeV at the 13 TeV Run 2 at LHC. Top-left panel shows V_1^0, top-right panel shows V_2^0, bottom-left panel shows V_1^+ and bottom-right panel shows V_2^+.

Despite the fact that we have introduced six new vector bosons, for g_V in the lower part of the allowed range only the heaviest, positively charged one is actually observable with the energy and integrated luminosity of Run 1 at the LHC. Its coupling being relatively weak, this particle resembles a heavy W' proposed in other contexts [24, 25, 27]. The main difference is that we predict the existence of five additional particles. In particular, the three V_1 particles have a mass that is 100 to 200 GeV smaller, and might have escaped detection because of suppressed couplings to SM fermions and hence suppressed production rates. On the other hand, for larger allowed values of g_V, for example $g_V \gtrsim 3$, both $V_1^+ \to W^+Z$ and $V_2^+ \to W^+h$ have cross-section times branching ratios around 4 fb, and hence might

provide a different, more conventional, explanation for the currently observed anomalies.

A distinctive feature of our model is that the new vectors couple to the SM fermions only via mixing with SM gauge bosons, as explained earlier. As a consequence, all the new charged vectors couple only to left-handed fermionic currents. This is atypical for W' models. The coupling of the neutral heavy vectors to the SM fermions depends on the value of g_V. For the smallest allowed values, the V_2^0 couples predominantly to left-handed fermionic currents and the V_1^0 couples to a left-right admixture.

In Fig. 7, we show the product of production cross section times branching ratio for the new particles with $\mu = 1.8$ TeV, but in collisions at 13 TeV. For large enough integrated luminosities, all the particles become visible, including V_1^+ and V_1^0. At the time in which we are editing this paper, the LHC collaborations are in the process of collecting data at 13 TeV center-of-mass energy: once their combined searches in leptonic as well as di-boson final states are published, it will be possible to draw exclusion regions in the (g_V, μ) plane, and test the viability of the present model.

7 Discussion

Motivated by tentative signals from the ATLAS and CMS experiments [1, 2] for high-mass resonant production of WW, WZ, ZZ and Wh pairs, we have developed a simple effective field theory that extends the standard model to include new vector resonances. A set of additional $SU(2)_{L'} \times SU(2)_{R'}$ gauge fields is included, preserving custodial electroweak symmetry in the new sector. The ingredients and structure of the EFT are shown in Table 1. The standard model sector of the EFT is described by the usual parameters: gauge couplings g and g', an electroweak-scale VEV f, and fermion Yukawa couplings. In addition, a left-right symmetric gauge coupling g_V and a vacuum expectation value $F \gg f$ characterize the new sector.

The structure of the EFT is explored keeping fixed the electroweak gauge-boson masses, the electroweak VEV $v_W \approx 246$ GeV, and the characteristic scale of new physics. This we take to range upward from the 2 TeV scale suggested by the ATLAS and CMS excesses. For each choice of this scale, the structure of the EFT then depends on one parameter, which we take to be g_V. It can a priori range from electroweak strength up to $\mathcal{O}(4\pi)$ where the new gauge bosons are strongly coupled. As g_V/g increases, the ratio F/f must decrease to keep fixed the scale of new physics $\mu = g_V F/2$. With this scale taken to be approximately 2 TeV, it turns out that at least one of the two conditions $f/F \ll 1$ or $g/g_V \ll 1$ must be met. Standard model precision physics, in particular the coupling of the Higgs boson to the $W^\pm$ then restricts the value of g_V to the range $g_V \lesssim 4.2$. By contrast, direct searches in leptonic channels lead to a lower bound $g_V \gtrsim 2.0$, for $\mu = 1.8$ TeV, in order to suppress adequately these branching fractions.

In the allowed region of parameter space, the model exhibits approximate parity doubling, in the sense that all the new vector bosons have masses that differ by no more than $100 - 200$ GeV, and similar widths. Furthermore, for g_V in the lower part of the range shown in Eq. (6.3), the heaviest charged resonance V_2^+ has a production cross section and di-boson branching fraction that could account for both the anomalies reported by ATLAS

and CMS, while lighter new particles, in particular the $V_1^{\pm}$, have a suppressed production cross section, putting them below observability at the LHC Run 1. By contrast, for $g_V \gtrsim 3$ the process $pp \to V_2^+ \to Wh$ and $pp \to V_1^+ \to WZ$ might separately be observable. These features of the model lead to the exciting prospect that future LHC exploration at higher energy and luminosity could reveal a rich phenomenology of heavy vector states.

To conclude, the model proposed and studied here is a simple representation of new physics that could arise at higher mass scales, such as the 2-TeV scale already accessible in Run 1 of the LHC. There, some possible excesses have been reported, and future studies in the 13 TeV Run 2 of the LHC could be even more interesting. The model could also describe new physics accessible only at these higher energies. We have used the mass scale 3 TeV in our model as an example of this. There, some of the bounds imposed on the parameters of our model would become weaker. Whatever the intrinsic scale of our model, it could originate microscopically in a variety of ways. While the coupling g_V is constrained to be relatively weak in our 2-TeV model, the underlying dynamics could be weakly coupled or strongly coupled, even at experimentally accessible energies.

Acknowledgments

We would like to thank Bogdan Dobrescu and Kenneth Lane for helpful discussions. The work of TA and JI is supported by the U. S. Department of Energy under the contract DE-FG02-92ER-40704. YB is supported by the U. S. Department of Energy under the contract DE-FG-02-95ER40896. The work of MP is supported in part by the STFC Consolidated Grant ST/J000043/1.

A Relation to Weinberg Sum Rules

The approach described here is in line with that often followed in the context of dynamical electroweak symmetry breaking. This amounts to computing current-current correlation functions in the new strongly-coupled sector responsible for electroweak symmetry breaking, and relating this to the propagators of the electroweak gauge bosons by assuming that the $SU(2)_L \times U(1)_Y$ gauge group is a subgroup of the symmetry group of the new sector. This maps onto our framework in the limit $g \ll g_V$, where $V_1 \approx (L+R)/\sqrt{2}$, $V_2 \approx (L-R)/\sqrt{2}$, and the new gauge-boson coupling is relatively strong.

A familiar expression for the S parameter in the Weinberg-sum-rule context is

$$S \equiv 4\pi \sum \left(\frac{f_\rho^2}{M_\rho^2} - \frac{f_{a_1}^2}{M_{a_1}^2} \right) , \tag{A.1}$$

where the sum is over all heavy spin-1 bosons, M_ρ and M_{a_1} are the masses of the vector and axial-vector resonances, respectively, while f_ρ and f_{a_1} are their decay constants.

In terms of Σ^+ (the current-current correlation function of the theory with $g = 0 = g'$) we find

$$\Sigma^+ \equiv F^2 + \frac{M_\rho^2 f_\rho^2}{2(q^2 - M_\rho^2)} + \frac{M_{a_1}^2 f_{a_1}^2}{2(q^2 - M_{a_1}^2)}\,, \tag{A.2}$$

where one can explicitly show that

$$M_\rho^2 = \frac{1}{4} g_V^2 F^2\,, \quad M_{a_1}^2 = \frac{1}{4} g_V^2 (F^2 + 2f^2)\,, \quad f_\rho^2 = \frac{F^2}{2}\,, \quad f_{a_1}^2 = \frac{F^4}{2(F^2 + 2f^2)}\,. \tag{A.3}$$

The first and second Weinberg sum rules follow :

$$f_{a_1}^2 - f_\rho^2 = -\frac{f^2 F^2}{F^2 + 2f^2} = -f_\pi^2\,, \tag{A.4}$$

$$M_{a_1}^2 f_{a_1}^2 - M_\rho^2 f_\rho^2 = 0\,. \tag{A.5}$$

The pion decay constant is defined in the body of the paper $\lim_{q\to 0} \Sigma^+ = \frac{f^2 F^2}{F^2 + 2f^2} = f_\pi^2$, where we identify it with the electroweak scale $f_\pi = v_W = 246$ GeV. Notice that this relation is actually exact, and does not rely on taking $g = 0$.

Using the above expressions, the $\hat{S}$ parameter becomes:

$$\hat{S} \equiv \frac{1}{4} g^2 \left(\frac{f_\rho^2}{M_\rho^2} - \frac{f_{a_1}^2}{M_{a_1}^2} \right) = \frac{g^2}{g_V^2} \frac{2f^2 (F^2 + f^2)}{(F^2 + 2f^2)^2}\,, \tag{A.6}$$

in agreement with Eq. (3.4), appropriate for the limit $g, g' \ll g_V$.

B Indirect Bounds from Higgs Physics

All the production and decay rates of the Higgs boson are affected by the way in which the couplings to the SM fields are suppressed in our model. We saw that the coupling to fermions is suppressed by the coefficient $c = v_W/f$. This suppression in turns affects the hgg coupling to the gluons that is responsible for the main contribution to the production cross-section of the Higgs particle,

$$\sigma(gg \to h) = c^2 \sigma(gg \to h)_{\rm SM}\,, \tag{B.1}$$

as well as the associated production with top quarks:

$$\sigma(pp \to ht\bar{t}) = c^2 \sigma(pp \to ht\bar{t})_{\rm SM}\,. \tag{B.2}$$

The same coupling c affects the decay rates into SM fermions, as well as gluons (via the top loop):

$$\Gamma(h \to \psi\bar{\psi}) = c^2\, \Gamma(h \to \psi\bar{\psi})_{\rm SM}\,, \tag{B.3}$$

$$\Gamma(h \to gg) = c^2\, \Gamma(h \to gg)_{\rm SM}\,. \tag{B.4}$$

The coupling to SM weak gauge bosons is suppressed by the factor a. It affects the production cross section of processes involving electroweak gauge bosons, such as vector-boson fusion and associated production with electroweak gauge bosons $V = W, Z$

$$\sigma(pp \to hjj) = a^2 \sigma(pp \to hjj)_{\rm SM}\,, \tag{B.5}$$
$$\sigma(pp \to Vh) = a^2 \sigma(pp \to Vh)_{\rm SM}\,. \tag{B.6}$$

It also affects the decay to pairs of electroweak gauge bosons:

$$\Gamma(h \to WW^*) = a^2\, \Gamma(h \to WW^*)_{\rm SM}\,, \tag{B.7}$$

and an analogous formula for ZZ^*.

Finally, the $h \to \gamma\gamma$ process is additionally affected by the Higgs coupling to heavy vectors, loops of which contribute to the $h \to \gamma\gamma$ amplitude. In the standard model the rate is dominated by the contribution of loops of heavy particles:

$$\Gamma(h \to \gamma\gamma)_{\rm SM} = \frac{G_F \alpha^2 m_h^3}{128\sqrt{2}\,\pi^3} \left| A_t(\tau_t) N_c N_f Q^2 \,+\, A_W(\tau_W) \right|^2 , \tag{B.8}$$

where $N_c = 3$, $N_f = 1$ and $Q = 2/3$ descend from the contribution of top loops, with $\tau_t = m_h^2/(4m_t^2)$ and

$$A_t(\tau_t) = \frac{2}{\tau_t^2} \left[\tau_t + (\tau_t - 1) \arcsin^2 \sqrt{\tau_t} \right] . \tag{B.9}$$

The contribution of W loops is controlled by

$$A_W(\tau_W) = -\frac{1}{\tau_W^2} \left[2\tau_W^2 + 3\tau_W + 3(2\tau_W - 1) \arcsin^2 \sqrt{\tau_W} \right] , \tag{B.10}$$

with $\tau_W = m_h^2/(4M_W^2)$. Notice that $A_W(\tau_W) \simeq -8.3$, while $A_W(0) = -7$. In our model, the rate is

$$\Gamma(h \to \gamma\gamma) = \frac{G_F \alpha^2 m_h^3}{128\sqrt{2}\,\pi^3} \left| c\, A_t(\tau_t) N_c N_f Q^2 \,+\, a\, A_W(\tau_W) \,+\, (c-a) A_W(0) \right|^2 , \tag{B.11}$$

where besides the modifications of the couplings to the top and photon, we include the loops of the two charged heavy vectors, and take the limit $M_{V_{1,2}} \gg m_h$. The couplings satisfy $a_1 + a_2 = c - a$.

The contribution of the di-photon channel to the total width is negligibly small. In the standard model the BR to WW^* or ZZ^* sum up to approximately 25%, while the remaining 75% comes primarily from bb, cc, $\tau\tau$ and gg, meaning that in our model the total width scales as

$$\frac{\Gamma}{\Gamma_{\rm SM}} \simeq 0.75\, c^2 \,+\, 0.25\, a^2\,. \tag{B.12}$$

References

[1] G. Aad *et al.* [ATLAS Collaboration], arXiv:1506.00962 [hep-ex].

[2] CMS Collaboration [CMS Collaboration], CMS-PAS-EXO-14-010.

[3] See for instance E. Accomando, L. Fedeli, S. Moretti, S. De Curtis and D. Dominici, Phys. Rev. D **86**, 115006 (2012) [arXiv:1208.0268 [hep-ph]], and references therein, in particular E. Accomando, S. De Curtis, D. Dominici and L. Fedeli, Phys. Rev. D **79**, 055020 (2009) [arXiv:0807.5051 [hep-ph]].

[4] K. Lane and A. Martin, Phys. Rev. D **80**, 115001 (2009) [arXiv:0907.3737 [hep-ph]].

[5] K. Lane and L. Prichett, arXiv:1507.07102 [hep-ph]; M. Low, A. Tesi and L. T. Wang, Phys. Rev. D **92**, no. 8, 085019 (2015) [arXiv:1507.07557 [hep-ph]]; D. B. Franzosi, M. T. Frandsen and F. Sannino, Phys. Rev. D **92**, 115005 (2015) doi:10.1103/PhysRevD.92.115005 [arXiv:1506.04392 [hep-ph]].

[6] N. Arkani-Hamed, A. G. Cohen and H. Georgi, Phys. Lett. B **513**, 232 (2001) [hep-ph/0105239]; N. Arkani-Hamed, A. G. Cohen, E. Katz, A. E. Nelson, T. Gregoire and J. G. Wacker, JHEP **0208**, 021 (2002) [hep-ph/0206020]; N. Arkani-Hamed, A. G. Cohen, E. Katz and A. E. Nelson, JHEP **0207**, 034 (2002) [hep-ph/0206021]; I. Low, W. Skiba and D. Tucker-Smith, Phys. Rev. D **66**, 072001 (2002) [hep-ph/0207243]; H. C. Cheng and I. Low, JHEP **0309**, 051 (2003) [hep-ph/0308199]. For a review see also M. Perelstein, Prog. Part. Nucl. Phys. **58**, 247 (2007) [hep-ph/0512128].

[7] T. Appelquist, H. C. Cheng and B. A. Dobrescu, Phys. Rev. D **64**, 035002 (2001) [hep-ph/0012100].

[8] B. Holdom, Phys. Lett. B **150**, 301 (1985); K. Yamawaki, M. Bando and K. i. Matumoto, Phys. Rev. Lett. **56**, 1335 (1986); T. W. Appelquist, D. Karabali and L. C. R. Wijewardhana, Phys. Rev. Lett. **57**, 957 (1986). For reviews see also R. S. Chivukula, hep-ph/0011264; K. Lane, hep-ph/0202255; C. T. Hill and E. H. Simmons, Phys. Rept. **381**, 235 (2003) [Phys. Rept. **390**, 553 (2004)] [hep-ph/0203079]; A. Martin, Subnucl. Ser. **46**, 135 (2011) [arXiv:0812.1841 [hep-ph]]; F. Sannino, Acta Phys. Polon. B **40**, 3533 (2009) [arXiv:0911.0931 [hep-ph]]; M. Piai, Adv. High Energy Phys. **2010**, 464302 (2010) [arXiv:1004.0176 [hep-ph]].

[9] M. Bando, T. Kugo, S. Uehara, K. Yamawaki and T. Yanagida, Phys. Rev. Lett. **54**, 1215 (1985); R. Casalbuoni, S. De Curtis, D. Dominici and R. Gatto, Phys. Lett. B **155**, 95 (1985); M. Bando, T. Kugo and K. Yamawaki, Phys. Rept. **164**, 217 (1988); H. Georgi, Nucl. Phys. B **331**, 311 (1990); M. Harada and K. Yamawaki, Phys. Rept. **381**, 1 (2003) [hep-ph/0302103].

[10] G. Aad *et al.* [ATLAS Collaboration], Phys. Lett. B **716**, 1 (2013) [arXiv:1207.7214 [hep-ex]].

[11] S. Chatrchyan *et al.* [CMS Collaboration], Phys. Lett. B **716**, 30 (2013) [arXiv:1207.7235 [hep-ex]].

[12] R. Barbieri, A. Pomarol, R. Rattazzi and A. Strumia, Nucl. Phys. B **703**, 127 (2004) [hep-ph/0405040].

[13] W. Buchmuller and D. Wyler, Nucl. Phys. B **268**, 621 (1986); Z. Han and W. Skiba, Phys. Rev. D **71**, 075009 (2005) [hep-ph/0412166].

[14] M. E. Peskin and T. Takeuchi, Phys. Rev. D **46**, 381 (1992).

[15] T. Appelquist and C. W. Bernard, Phys. Rev. D **22**, 200 (1980); A. C. Longhitano, Phys. Rev. D **22**, 1166 (1980); Nucl. Phys. B **188**, 118 (1981); T. Appelquist and G. H. Wu, Phys. Rev. D **48**, 3235 (1993) [hep-ph/9304240]; T. Appelquist and G. H. Wu, Phys. Rev. D **51**, 240 (1995) [hep-ph/9406416].

[16] A. Carmona, A. Delgado, M. Quirós and J. Santiago, JHEP **1509**, 186 (2015) [arXiv:1507.01914 [hep-ph]].

[17] M. Fabbrichesi, M. Pinamonti, A. Tonero and A. Urbano, arXiv:1509.06378 [hep-ph].

[18] M. B. Einhorn and D. R. T. Jones, Phys. Rev. D **46**, 5206 (1992).

[19] The ATLAS and CMS Collaborations, ATLAS-CONF-2015-044.

[20] A. D. Martin, W. J. Stirling, R. S. Thorne and G. Watt, Eur. Phys. J. C **63**, 189 (2009) [arXiv:0901.0002 [hep-ph]].

[21] S. Dawson, Nucl. Phys. B **249**, 42 (1985); Z. Kunszt and D. E. Soper, Nucl. Phys. B **296**, 253 (1988); D. Pappadopulo, A. Thamm, R. Torre and A. Wulzer, JHEP **1409**, 060 (2014) [arXiv:1402.4431 [hep-ph]].

[22] G. Aad *et al.* [ATLAS Collaboration], JHEP **1409**, 037 (2014) [arXiv:1407.7494 [hep-ex]].

[23] G. Aad *et al.* [ATLAS Collaboration], Phys. Rev. D **90**, no. 5, 052005 (2014) [arXiv:1405.4123 [hep-ex]].

[24] A. Thamm, R. Torre and A. Wulzer, arXiv:1506.08688 [hep-ph].

[25] J. Brehmer, J. Hewett, J. Kopp, T. Rizzo and J. Tattersall, arXiv:1507.00013 [hep-ph].

[26] B. C. Allanach, B. Gripaios and D. Sutherland, Phys. Rev. D **92**, no. 5, 055003 (2015) [arXiv:1507.01638 [hep-ph]].

[27] K. Cheung, W. Y. Keung, P. Y. Tseng and T. C. Yuan, arXiv:1506.06064 [hep-ph]; B. A. Dobrescu and Z. Liu, arXiv:1506.06736 [hep-ph]; Y. Gao, T. Ghosh, K. Sinha and J. H. Yu, Phys. Rev. D **92**, no. 5, 055030 (2015) [arXiv:1506.07511 [hep-ph]]; Q. H. Cao, B. Yan and D. M. Zhang, arXiv:1507.00268 [hep-ph]; B. A. Dobrescu and Z. Liu, JHEP10(2015)118 [arXiv:1507.01923 [hep-ph]]; L. Bian, D. Liu and J. Shu, arXiv:1507.06018 [hep-ph]; P. S. Bhupal Dev and R. N. Mohapatra, Phys. Rev. Lett. **115**, no. 18, 181803 (2015) [arXiv:1508.02277 [hep-ph]].